Geometrical effect on the non-Abelian spin-orbital gauge field of a curved surface

Tai-Chung Cheng
Municipal Zhung-Lun High School, Taipei, Taiwan

Jiann-Yeu Chen
Center of Nanoscience & Nanotechnology, National Chung Hsing University, Taichung, Taiwan

Ching-Ray Chang*
National Taiwan University, Taipei 10617, Taiwan

(Received 30 August 2010; revised manuscript received 7 March 2011; published 16 December 2011)

The geometrical effect of a two-dimensional electron gas system with the Rashba and Dresselhaus spin-orbital interactions on a curved surface is studied; it corresponds to a non-Abelian gauge field and a scalar field. The behavior of electrons with spin on a curved space can be transformed into that of a simple system of an electron with spin on a flat surface with a geometrical metric tensor. In addition to the dynamic phase of traveling electrons on a flat surface, a geometrical phase induced by curved space is also observed, and this phase can be demonstrated by use of the path integral. Therefore, the spin-rotation operator and quantum loop of electrons with spin on a curved space are obtained. The induced phases on three curved spaces with flat, cylindrical, and spherical geometry are calculated, and the roles of space curvature in spin precession are also analyzed.

DOI: 10.1103/PhysRevB.84.214423 PACS number(s): 72.25.Dc, 71.70.Ej, 73.23.−b

I. INTRODUCTION

The spin-orbital (SO) interaction in a two-dimensional electron gas (2DEG) has attracted great interest not only for its profound fundamental spin physics but also for its wide applications in spintronic devices.[1,2] The dominant SO couplings in planar semiconductor heterostructures are the Rashba and Dresselhaus effects, and they offer possibilities of controlling the spin without an external magnetic field. The former is due to structure inversion asymmetry,[3,4] which can be adjusted by the gate voltage,[5–8] while the latter is due to bulk inversion asymmetry[9] with its strength being material specific.

Earlier studies[10,11] showed that SO coupling including the Rashba and Dresselhaus terms can be regarded as a non-Abelian gauge field SU(2), or the Yang-Mills field.[12] The SU(2) gauge field is due to the spin-dependent phase of the traversing electrons. The spin-dependent phase depends only on the track of the path and is independent of the traveling speed of the electrons. Therefore it is usually called the geometrical phase or Berry phase.[13] The linkage of the SO interaction and the non-Abelian SU(2) gauge offers an elegant method to study a lot of interesting physical phenomena in 2DEGs, such as the persistent spin helix and spin filter.[10,14,15] Complicated spin dynamics due to the spin-orbit coupling can then be easily understood in terms of a theory where the coupling is treated as a non-Abelian gauge field, and the corresponding formalism can be used to study the single-electron spin transport in 2DEGs and spin manipulation in quantum dot systems.[15–24]

When applied to the 2DEG, the approach based on a formal SU(2) gauge invariance of the spin-orbit Hamiltonian proved that the equilibrium spin current can be gauged away if the spin-orbital field is a pure gauge.[25] Until now, most studies of the spin electrons have been concentrated on planar 2D systems.[26] However, there are also a number of studies on the behavior of electrons on a specific shape of 2D surface, such as cylindrical[27–29] and spherical[30,31] surfaces. Curved 2D systems have attracted a lot of recent interest,[27–31] and the Rashba spin-orbital interaction (RSI) and Dresselhause spin-orbital interaction (DSI) have been used to study electrons on a cylindrical surface.[32] Even though a lot of experiments on spin transport in nanotubes and nanopillars have been carried out, only a few theoretical studies on the Hamiltonian with RSI and DSI on a curved surface have been presented.[33] The reported results indicate that the geometrical effects on spin-polarized electrons in a curved space cannot be neglected, and the exact analysis of electrons with spin on a curved surface deserves further studies. In particular, it remains to be clarified whether or not the spin-orbit field can still be completely removed by a gauge transformation on a curved surface.[25] To fully understand the behavior of electrons with spin in a 2DEG with a curved space, the geometrical effect on spin-polarized electrons on a curved surface is another important effect of spin-polarized electrons to be clarified, besides the spin-dependent geometrical phase on a flat surface.

Here we take into account a curved surface which is endowed with a metric tensor, and we can explicitly study the non-Abelian spin-orbital gauge field on all kinds of two-dimensional topological surfaces. In other words, the travel of electrons with spin on any curved surfaces can be mapped into a flat planar structure with the help of the geometrical metric tensor. This paper is organized as follows. In Sec. II we construct the non-Abelian spin-orbital gauge field on curved surfaces. Based on the Hamiltonian with Rashba and Dresselhaus spin-orbital interactions on a curved surface, the spin-rotation operator and quantum loop are derived by use of the path integral. A linear approximation of space curvature is used in Sec. III, and the geometrical effect of curvature can be rigorously treated as a weak-field correction on a flat surface. In Sec. IV we study the behavior of spin precession on curved surfaces, and two examples are explicitly examined.

As the curvature of the curved space increases, the precession period of spin-polarized electrons varies, suggesting that the spin-polarized electrons experienced an additional effective geometric field due to the surface curvature. Also, the different behavior of electrons with spin traveling on flat, cylindrical, and spherical surfaces clearly shows the role of the space curvature. Finally, the conclusions are given in Sec. V.

II. FORMALISM ON A CURVED SPACE

The Hamiltonian of an electron with the RSI (Refs. 5 and 34) and DSI (Refs. 35 and 36) in three dimensions is given by

$$H = \frac{p^2}{2m} + \frac{\alpha}{\hbar}(\vec{\sigma} \times \vec{p}) \cdot \hat{n} - \frac{\beta}{\hbar}\vec{\sigma} \cdot \vec{\chi} \tag{1}$$

with

$$\vec{\chi} = \begin{pmatrix} 2n_x(n_y p_y - n_z p_z) + \left(n_y^2 - n_z^2\right) p_x \\ 2n_y(n_z p_z - n_x p_x) + \left(n_z^2 - n_x^2\right) p_y \\ 2n_z(n_x p_x - n_y p_y) + \left(n_x^2 - n_y^2\right) p_z \end{pmatrix} \tag{2}$$

(see Appendix A).

In order to study the geometrical effect induced by a curved surface, we assume that the spin-polarized electron is constrained on a 2D curved surface with normal unit vector. For the general case with the curved surface given by $z = (x, y)$, we substitute $z = (x, y)$ into Eq. (1), and the Hamiltonian can be generalized into a curved surface of the form

$$H = \frac{1}{2m} p_\mu p^\mu - \frac{e}{mc}\{A_\mu, p^\mu\}_H. \tag{3}$$

Here we use the Einstein summation and metric tensor to define Eq. (3) (see Appendix B). Furthermore, Eq. (3) can be expressed in the quadratic form

$$H = \frac{1}{2m}\left(p - \frac{e}{c}A\right)_\mu \left(p - \frac{e}{c}A\right)^\mu + e\Phi, \tag{4}$$

where A_μ and Φ are function of position and Φ is defined by

$$\Phi = -\frac{e}{2mc^2} A^i_\mu A^{i\mu}. \tag{5}$$

The Hamiltonian of the curved surface can be transformed into a generalized Hamiltonian describing a particle subjected to an SU(2) gauge field A_μ and a scalar field Φ on a plane, as shown in Fig. 1. Hereafter, the generalized Hamiltonian is considered throughout this paper.

By applying the path-integral method, the wave function can be obtained:

$$\psi\left(r_f^\mu, t_f\right) = N\left(\int DxU_D U_G\right)\psi\left(r_i^\mu, t_i\right). \tag{6}$$

N is a normalization factor. The integration represents the sum of contributions over all paths that connect the initial wave function $\psi(r_i^\mu, t_i)$ and the final wave function $\psi(r_f^\mu, t_f)$, weighted by U_D and U_G. U_D is the usual dynamical phase given by

$$U_D = \exp\left(-\frac{i}{\hbar}\int \frac{m}{2} v_\mu v^\mu - e\Phi dt\right), \tag{7}$$

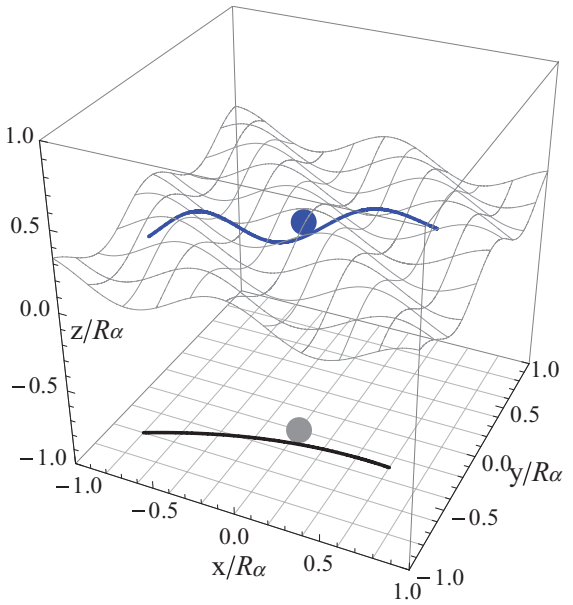

FIG. 1. (Color online) A curved space in x-y-z coordinates and the contour on curved space projected on the x-y plane. An electron with SO interaction on a curved surface can be described with an SU(2) gauge field and a scalar field on the x-y plane.

and U_G is the geometrical phase,

$$U_G = P\exp\left(\frac{ie}{\hbar c}\int A_\mu dr^\mu\right). \tag{8}$$

P stands for the path order, because the integral depends entirely on the path taken from the initial position r_i^μ to the final position r_f^μ. Here we derived the non-Abelian geometric phase by gauge transformation and the path integral. The exact same results can also be obtained by the adiabatic approximation[37] for our system. In other cases, the identical results derived by adiabatic approximation and the path integral for both the non-Abelian[37] and Abelian[38] geometric phases have been reported. In addition, U_G can be regarded as a gauge transformation of

$$U_G H U_G^+ = H_D \tag{9}$$

which maps H to H_D. H_D is given by

$$H_D = \frac{1}{2m} p_\mu p^\mu + e\Phi. \tag{10}$$

By comparison with the rotation operator for a two-component spinor, U_G can be regarded as a series of infinitesimal rotations (see Appendix C) such as

$$U_G = P\prod_k^\infty \exp\left(-\frac{i}{2}\sigma_j n^j d\varphi\right)_k, \tag{11}$$

which rotate about

$$n^i = \pm A^i_\mu \frac{dr^\mu}{ds}\left(A^j_\rho A^j_\sigma \frac{dr^\rho}{ds}\frac{dr^\sigma}{ds}\right)^{-\frac{1}{2}} \tag{12}$$

with the angle

$$d\varphi = \frac{\pm 2e}{\hbar c}\left(A^j_\mu A^j_\nu \frac{dr^\mu}{ds}\frac{dr^\nu}{ds}\right)^{\frac{1}{2}} ds. \tag{13}$$

With the same product of n^i and $d\varphi$ in Eq. (11), the same sign in Eqs. (12) and (13) should be chosen.

In order to study the spin motion of traveling electrons, we seek for the spin evolution after a distance on curved surfaces. The expectation value of the spin can be obtained by a series of infinitesimal rotations as

$$\langle S(x^\mu)\rangle_i = R_i^j \left\langle S\left(x_0^\mu\right)\right\rangle_j . \tag{14}$$

The rotation matrix for the spin components is

$$R_i^j = P\prod_k^\infty (1 + J\,d\varphi)_k \tag{15}$$

where the J generator is given by

$$J = \begin{pmatrix} 0 & -n_z & n_y \\ n_z & 0 & -n_x \\ -n_y & n_x & 0 \end{pmatrix}. \tag{16}$$

Note that the path-order product reduces to the ordinary product as long as all gauge fields A_μ on the traversing path satisfy the commutation relation

$$\left(A_\mu \frac{dr^\mu}{ds}, A'_\nu \frac{dr'^\nu}{ds}\right) = 0. \tag{17}$$

Thus, the rotation operator reduces to the ordinary exponential form as

$$U_G = \exp\left(-\frac{i}{2}\sigma_j n^j \Delta\varphi\right), \tag{18}$$

which rotates about the direction

$$n^i = \pm\left(\int A_\mu^i \frac{dr^\mu}{ds} ds\right)\left(\int A_\mu^j \frac{dr^\mu}{ds} ds \int A_\nu^j \frac{dr^\nu}{ds} ds\right)^{-\frac{1}{2}} \tag{19}$$

with angle

$$\Delta\varphi = \frac{\pm 2e}{\hbar c}\left(\int A_\mu^i \frac{dr^\mu}{ds} ds \int A_\nu^i \frac{dr^\nu}{ds} ds\right)^{\frac{1}{2}}. \tag{20}$$

The rotation matrix for the spin components can then be simplified into

$$R_i^j = \begin{pmatrix} n_x^2 + \left(1 - n_x^2\right)\cos\varphi & n_x n_y(1-\cos\varphi) - n_z\sin\varphi & n_x n_z(1-\cos\varphi) + n_y\sin\varphi \\ n_x n_y(1-\cos\varphi) + n_z\sin\varphi & n_y^2 + \left(1 - n_y^2\right)\cos\varphi & n_y n_z(1-\cos\varphi) - n_x\sin\varphi \\ n_x n_z(1-\cos\varphi) - n_y\sin\varphi & n_y n_z(1-\cos\varphi) + n_x\sin\varphi & n_z^2 + \left(1 - n_z^2\right)\cos\varphi \end{pmatrix}. \tag{21}$$

The spin-orbit interaction can be regarded as a non-Abelian gauge field and therefore the quantum square ring[11,39] can be derived as in the standard process of the Wilson loop[41] (see Appendix D).

III. EFFECTIVE GEOMETRIC FIELD

In general relativity, the curved space and gravitational field are equivalent from the equivalence principle.[42] Similarly, the spin-orbital coupling on a slightly curved space can also be treated as a geometric field. When the curvature radius of the curved space is much larger than the electron wavelength, a semiclassical approximation with the Taylor expansion of the Hamiltonian only to the first order in $\partial_x z$ and $\partial_y z$ can be justified. For a GaAs/AlGaAs system,[43] the electron wavelength is about 10^{-8} m, and the curvature radius of the reported[43] cylindrical GaAs/AlGaAs is around 10^{-6} m; therefore, the semiclassical approximation in this section is valid. H can be decomposed into a combination of two effective Hamiltonians and the higher-order corrections

$$H = H_0 + H_{G1} + O(2). \tag{22}$$

H_0 is the spin-orbital Hamiltonian on a flat surface,

$$H_0 = \frac{1}{2m}\left(p_x^2 + p_y^2\right) + \frac{\alpha}{\hbar}(\sigma_x p_y - \sigma_y p_x) + \frac{\beta}{\hbar}(\sigma_x p_x + \sigma_y p_y), \tag{23}$$

and H_{G1} is the first-order geometrical correction written as

$$H_{G1} = \frac{\sigma_z}{\hbar}(-\alpha\partial_y z + 2\beta\partial_x z)p_x + (\alpha\partial_x z - 2\beta\partial_y z)p_y, \tag{24}$$

which can be regarded as coming from an effective geometric field. In general, the effective geometric field on a slightly curved space cannot be removed through a particular gauge; instead, it can be expressed as a geometrical induced field,

$$B_{G1} = \frac{2mc}{e\hbar^2}(0,0,\alpha(-\partial_y z p_x + \partial_x z p_y) + 2\beta(\partial_x z p_x - \partial_y z p_y)). \tag{25}$$

It is interesting to notice that the geometrical induced field will be only perpendicular to the x-y plane. This geometrical induced field is very different from the effective B_0 field induced from RSI and DSI in U(1),where

$$B_0 = \frac{2mc}{e\hbar^2}(\alpha p_y + \beta p_x, -\alpha p_x + \beta p_y, 0). \tag{26}$$

B_{G1} is only along the z axis and also linearly depends on the curvature of the surface, while B_0 is always in plane. It should be noted that the eigenspinor will gradually switch out of the in-plane direction for the geometrical induced field B_{G1}.

The Hamiltonian can be rewritten as a free electron experiencing two gauge fields and one scalar field:

$$H = \frac{1}{2m}\left[p - \frac{e}{c}(A_0 + A_{G1})\right]_\mu \left[p - \frac{e}{c}(A_0 + A_{G1})\right]^\mu + e\Phi + O(2). \tag{27}$$

One of the non-Abelian gauges is the conventional spin-orbital $A_{\mu 0}$ in flat space[15] given by

$$A_{0\mu} = \sigma_i A^i_{0\mu}, \tag{28}$$

where

$$\begin{aligned} A^1_{0\mu} &= \frac{mc}{e\hbar}(-\beta, -\alpha), \\ A^2_{0\mu} &= \frac{mc}{e\hbar}(\alpha, \beta), \\ A^3_{0\mu} &= 0, \end{aligned} \tag{29}$$

and the other is $A_{G1\mu}$, which is a new non-Abelian gauge induced by the curved surface and is given by

$$A_{G1\mu} = \sigma_i A^i_{G1\mu}, \tag{30}$$

where

$$\begin{aligned} A^1_{G1\mu} &= A^2_{G2\mu} = 0, \\ A^3_{G1\mu} &= \frac{mc}{e\hbar}(\alpha\partial_y z - 2\beta\partial_x z, -\alpha\partial_x z + 2\beta\partial_y z). \end{aligned} \tag{31}$$

Φ is a field given by

$$\Phi = \frac{m}{\hbar}(\alpha^2 + \beta^2), \tag{32}$$

which is a constant field when α and β are position independent. The two non-Abelian gauge fields are not scalar fields and their components do not commute. The noncommutability makes the usual scalar gauge formalism inapplicable and complicates the problem. However, as an interesting exceptional case with equal strengths of the RSO and the DSO couplings on a flat surface,[15] there also exist some special pure gauge couplings in slightly curved space discussed here. Two gauge fields can be simultaneously removed when (a) $\alpha = \beta$ and $\partial_x z = \partial_y z$ or (b) $\alpha = -\beta$ and $\partial_x z = -\partial_y z$, and the spin-orbital coupling system can then be transformed into a free-electron system.The commutator also vanishes for a one-dimensional system.[15]

The rotation operator for a two-component spinor can be divided into two kinds of rotation:

$$U_G = P\prod_k^\infty \exp\left(-\frac{i}{2}\sigma_j n^j_0 d\varphi_0\right)_k \exp\left(-\frac{i}{2}\sigma_l n^l_{G1} d\varphi_{G1}\right)_k. \tag{33}$$

One of the rotation operations is in flat space with the rotation axis

$$\begin{aligned} n^i_0 = \pm &\left(\beta\frac{dx}{ds} + \alpha\frac{dy}{ds}, -\alpha\frac{dx}{ds} - \beta\frac{dy}{ds}, 0\right) \\ &\times \left\{(\alpha^2+\beta^2)\left[\left(\frac{dx}{ds}\right)^2 + \left(\frac{dy}{ds}\right)^2\right] + \alpha\beta\frac{dx}{ds}\frac{dy}{ds}\right\}^{-\frac{1}{2}} \end{aligned} \tag{34}$$

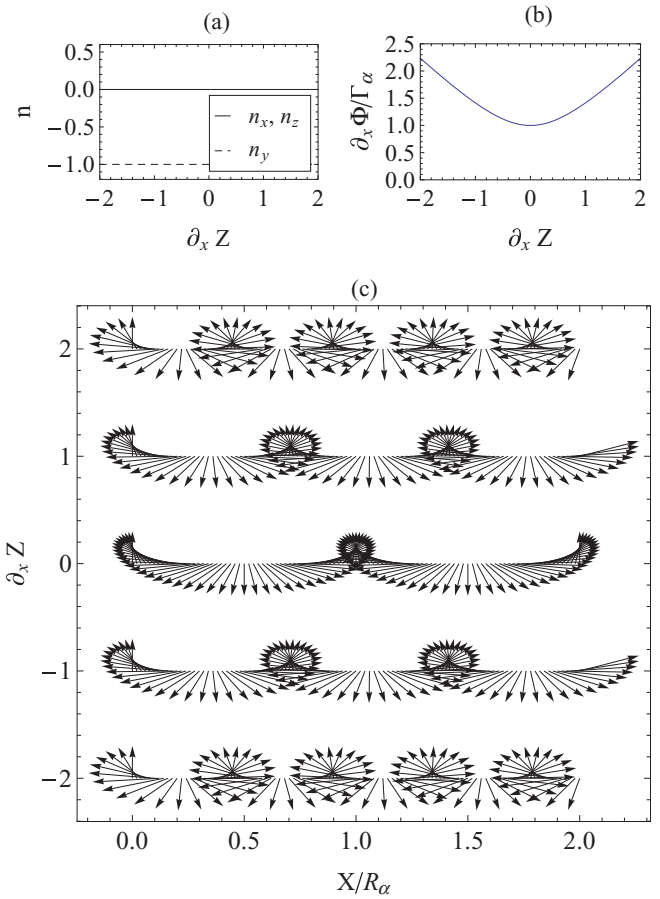

FIG. 2. (Color online) Spin precession with longitudinal slope and pure Rashba coupling. (a) The unit vector along the rotation axis is a function of slope $\partial_x z$. (b) $\partial_x\phi$ depends on $\partial_x z$ and $\Gamma_\alpha = 2m\alpha/\hbar^2$. (c) Rashba spin precession is along the x direction with $\partial_x z = -2, -1, 0, 1, 2$, and the other parameters are fixed, i.e., $\beta = 0$, $\partial_y z = 0$, and $R_\alpha = \pi\hbar^2/m\alpha$.

and the rate of change of the precession angle with respect to the displacement

$$\frac{d\varphi_0}{ds} = \frac{\pm 2m}{\hbar^2}\left\{(\alpha^2+\beta^2)\left[\left(\frac{dx}{ds}\right)^2 + \left(\frac{dy}{ds}\right)^2\right] + \alpha\beta\frac{dx}{ds}\frac{dy}{ds}\right\}^{\frac{1}{2}}. \tag{35}$$

The other rotation operation from the geometrical correction is along the rotation axis,

$$n^i_{G1} = \pm(0,0,1), \tag{36}$$

and the rate of change of the precession angle is

$$\begin{aligned} \frac{d\varphi_{G1}}{ds} = \frac{\pm 2m}{\hbar^2}\Bigg[&\left((\alpha\partial_y z - 2\beta\partial_x z)\frac{dx}{ds}\right)^2 \\ &+ \left((-\alpha\partial_x z + 2\beta\partial_y z)\frac{dx}{ds}\right)^2\Bigg]^{\frac{1}{2}}. \end{aligned} \tag{37}$$

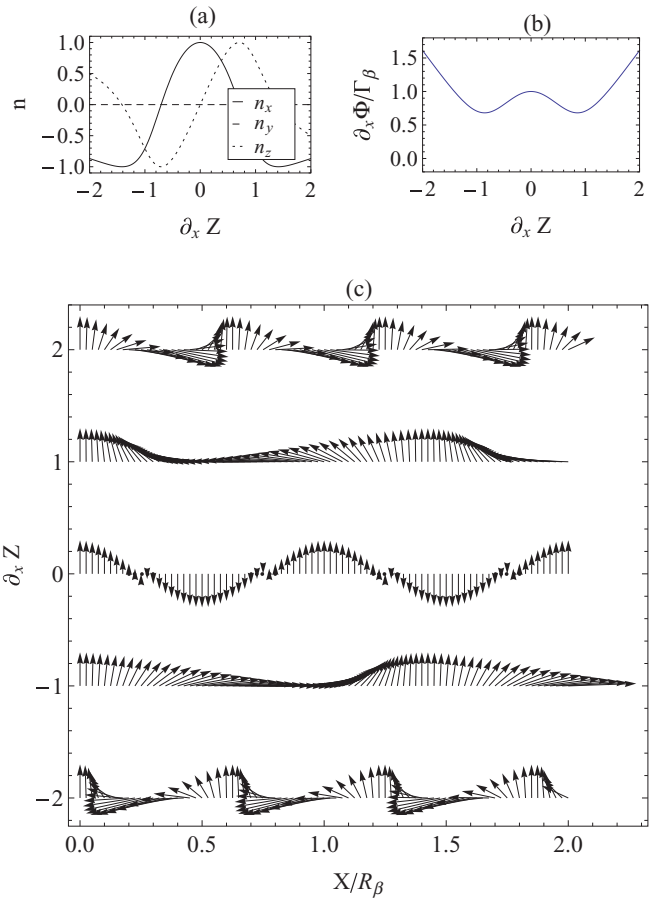

FIG. 3. (Color online) Spin precession with longitudinal slope and pure Dresselhaus coupling. (a) The unit vector along the rotation axis is a function of slope $\partial_x z$. (b) $\partial_x \phi/\Gamma_\beta$ as a function of $\partial_x z$ and $\Gamma_\beta = 2m\beta/\hbar^2$. (c) Dresselhaus spin precession is along the x direction with $\partial_x z = -2,-1,0,1,2$, and the other parameters are fixed as $\partial_y z = 0$ and $R_\beta = \pi\hbar^2/m\beta$.

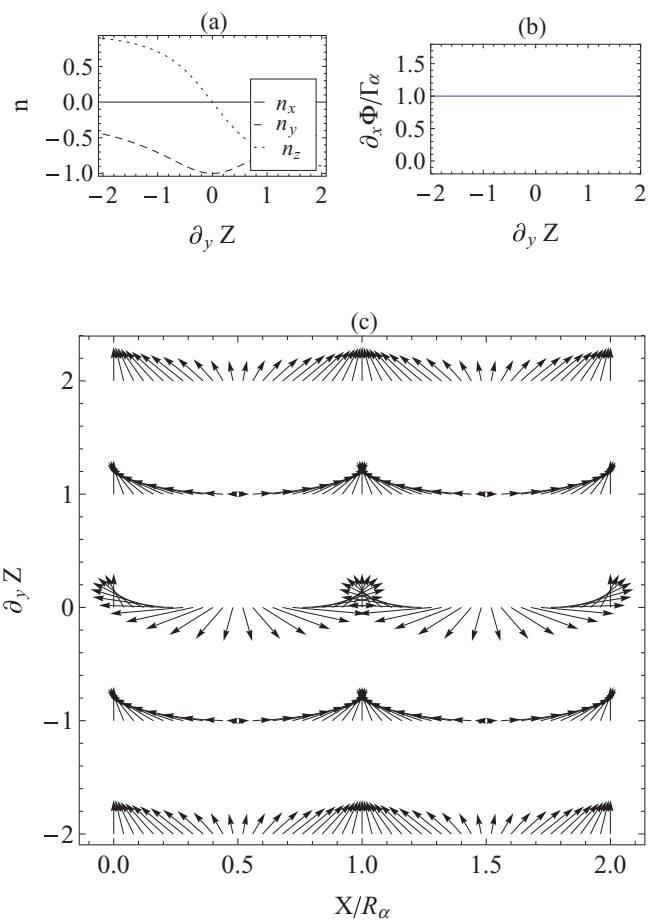

FIG. 4. (Color online) Spin precession with transverse slope and pure Rashba coupling. (a) The unit vector along the rotation axis is a function of slope $\partial_y z$. (b) $\partial_x \phi/\Gamma_\alpha$ as a function of $\partial_y z$ and $\Gamma_\alpha = 2m\alpha/\hbar^2$. (c) Rashba spin precession is along the x direction with $\partial_y z = -2,-1,0,1,2$, and the other parameters are fixed as $\partial_x z = 0$ and $R_\alpha = \pi\hbar^2/m\alpha$.

The rotation matrix for spin components becomes

$$R_i^j = P\prod_k^\infty [1 + (J_0 + J_{G1})\, d\varphi]_k \,. \tag{38}$$

J_0 is the generator in flat space given by

$$J_0 = \left\{(\alpha^2+\beta^2)\left[\left(\frac{dx}{ds}\right)^2 + \left(\frac{dy}{ds}\right)^2\right] + \alpha\beta\frac{dx}{ds}\frac{dy}{ds}\right\}^{-\frac{1}{2}} \times \begin{pmatrix} 0 & 0 & -\alpha\frac{dx}{ds} - \beta\frac{dy}{ds} \\ 0 & 0 & -\beta\frac{dx}{ds} - \alpha\frac{dy}{ds} \\ \alpha\frac{dx}{ds} + \beta\frac{dy}{ds} & \beta\frac{dx}{ds} + \alpha\frac{dy}{ds} & 0 \end{pmatrix} \tag{39}$$

and the geometrical correction is

$$J_{G1} = \begin{pmatrix} 0 & 1 & 0 \\ -1 & 0 & 0 \\ 0 & 0 & 0 \end{pmatrix}. \tag{40}$$

IV. SPIN PRECESSIONS ON CURVED SPACES

We now consider the spin precession for spin-polarized electrons with Rashba and Dresselhaus interactions on curved surfaces. Note that all geometrical information about the two-dimensional space is contained in the metric tensor. The metric tensor is dominated only by $\partial_x z$ and $\partial_y z$ [see Appendix A, Eq. (A2)]. Therefore, we can analyze the geometrical effect on spin precession due to $\partial_x z$ and $\partial_y z$. Now, we consider only the spin precession along the x axis (where we denote by x and y the longitudinal and transverse directions, respectively) and analyze its rotation angle φ and unit vector along the rotation axis under the following two conditions.

A. Longitudinal slope

In the special case with the influences of only the slope $\partial_x z$ and RSI, considering the electron with spin polarized along the z axis (z polarized) and propagating along the x axis with different slopes $\partial_x z = -2,-1,0,1,2$, the spin precession projected on the x-y plane is shown in Fig. 2. The spin precession can be realized by considering the rotation axis and angle. The rotation axis is along the unit vector

$$n = \pm(0,-1,0), \tag{41}$$

which is independent of slope. The + sign is arbitrarily chosen and shown in Fig. 2(a). The rate of change of the precession angle with respect to x is given by

$$\frac{d\varphi}{dx} = \frac{\pm 2m\alpha}{\hbar^2}[1 + (\partial_x z)^2]^{\frac{1}{2}}, \tag{42}$$

which increases as the slope $\partial_x z$ becomes steeper. The + sign is also chosen and shown in Fig. 2(b). Alternatively, we can simplify the equation by substituting $ds = (dx^2 + dy^2)^{1/2}$ into Eq. (42); thus the change of angle with the displacement is independent of the slope, but proportional to the travel distance. The spin orientation depends only on the magnitude of the slope and is symmetric with respect to the slope. The smallest rate of change of the precession angle is for the flat surface and is $\frac{2m\alpha}{\hbar^2}$. From Fig. 2(c), the larger the absolute value of the slope, the shorter the precession period of the spinning electrons, and this suggested that a larger effective Rashba field is applied on the spinning electrons under a large slope of the curved surface.

In a case with influences of only the slope $\partial_x z$ and DSI, also considering a z-polarized electron propagating along the x axis with different slopes $\partial_x z = -2, -1, 0, 1, 2$, the spin procession projected on the x-y plane is shown in Fig. 3. The unit vector of the spin-rotation axis is

$$n = \pm\left(\frac{1 - 2(\partial_x z)^2}{\{[1 - 2(\partial_x z)^2]^2 + [2\partial_x z - (\partial_x z)^3]^2\}^{\frac{1}{2}}}, 0, \frac{2\partial_x z - (\partial_x z)^3}{\{[1 - 2(\partial_x z)^2]^2 + [2\partial_x z - (\partial_x z)^3]^2\}^{\frac{1}{2}}}\right). \tag{43}$$

The + sign is chosen and shown in Fig. 3(a). Instead of the constant vector in the RSI, the spin-orientation axis varies with the increasing slope.

The rate of change of the precession angle with respect to x is

$$\frac{d\varphi}{dx} = \frac{\pm 2m\beta}{\hbar^2}\frac{\{[1 - 2(\partial_x z)^2]^2 + [2\partial_x z - (\partial_x z)^3]^2\}^{\frac{1}{2}}}{1 + (\partial_x z)^2}. \tag{44}$$

The + sign is chosen and shown in Fig. 3(b). Note that there is one local maximum at $\partial_x z = 0$ and two minima at $\partial_x z = \pm 1$. Therefore, the precession varies more slowly when the slope equals ± 1 as shown in Fig. 3(c). It is noted that on a flat surface the rate of change of the precession angle is $2m\beta/\hbar^2$ and is comparatively larger than that on a slightly curved surface. The rate of change of the precession angle reaches a minimal value of $\sqrt{2}m\beta/\hbar^2$ at $\partial_x z = \pm 1$; this indicates that in the DSI contribution the effective field induced by the curved space is smaller than that from the flat surface. The spin-rotation axis also changes from the (1,0,0) direction of the flat surface to $\pi/2$ at the curved surface when $\partial_x z = \pm 1$.

B. Transverse slope

In a case with only the slope $\partial_y z$ and RSI, considering a z-polarized electron propagating along the x axis with different slopes $\partial_y z = -2, -1, 0, 1, 2$, the spin procession projected on the x-y plane is shown in Fig. 4. The rotation axis is along the unit vector

$$n = \pm\left(0, \frac{-1}{[1 + (\partial_y z)^2]^{\frac{1}{2}}}, \frac{-\partial_y z}{[1 + (\partial_y z)^2]^{\frac{1}{2}}}\right). \tag{45}$$

The + sign is chosen and shown in Fig. 4(a). The rate of change of the precession angle with respect to x is constant and given by

$$\frac{d\phi}{dx} = \frac{\pm 2m\alpha}{\hbar^2}; \tag{46}$$

the + sign is chosen and shown in Fig. 4(b).

The rate of change of the precession angle is always constant, whether the 2DEG surface is flat or not. This suggests that the rate of precession along the x direction in RSI

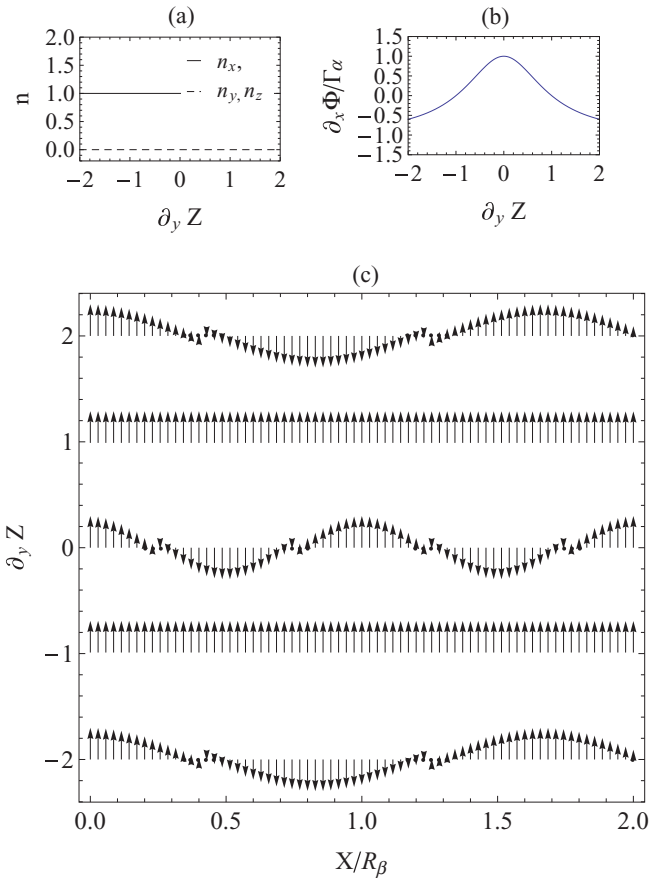

FIG. 5. (Color online) Spin precession with transverse slope and pure Dresselhaus coupling. (a) The unit vector along the rotation axis is a function of slope $\partial_y z$. (b) $\partial_x\phi/\Gamma_\beta$ as a function of $\partial_y z$ and $\Gamma_\beta = 2m\beta/\hbar^2$. (c) Dresselhaus spin precession is along the x direction with $\partial_y z = -2, -1, 0, 1, 2$, and the other parameters are fixed as $\partial_x z = 0$ and $R_\beta = \pi\hbar^2/m\beta$.

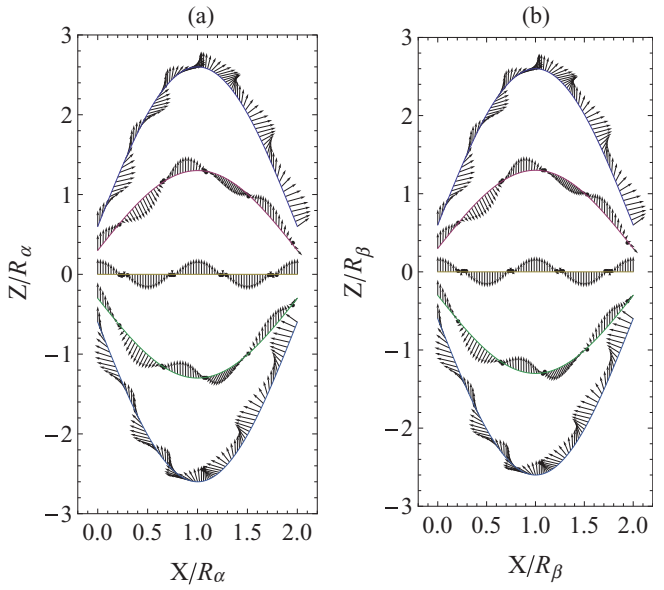

FIG. 6. (Color online) Precession along a curved path $z(x) = A\sin(\pi x/L)$. (a) is pure Rashba and (b) is pure Dresselhaus spin-orbital coupling, and $R_\alpha = \pi\hbar^2/m\alpha, R_\beta = \pi\hbar^2/m\beta$, respectively.

depends only on the x slope on a curved space. However, the spin-rotation axis varies only as the slope changes along the y direction. This suggested that if only RSI exists within a 2DEG system, the curvature along the y direction does not modify the effective strength of the geometric field; instead, it changes only the direction of the geometrical field. The spin-rotation angle approaches the z axis as the slope increases.

In a case with only the slope $\partial_y z$ and DSI, considering a z-polarized electron propagating along the x axis with different slopes $\partial_y z = -2,-1,0,1,2$, the spin precession projected on the x-y plane is shown in Fig. 5(c). The unit vector of the spin-rotation axis is

$$n = \pm(1,0,0). \tag{47}$$

The + sign is chosen and shown in Fig. 5(a). The rate of change of the precession angle with respect to x is

$$\frac{d\varphi}{dx} = \frac{\pm 2m\beta}{\hbar^2}\frac{1-(\partial_y z)^2}{1+(\partial_y z)^2}. \tag{48}$$

The + sign is chosen and shown in Fig. 5(b). Note that the precession is frozen when $\partial_y z = \pm 1$ and this means that one can make a curved surface without the spin precession of the transport electrons. Similar frozen behavior of spin electrons was reported in spin transport wires.[39]

C. Two examples

Based on the previous discussion, the slopes $\partial_x z$ and $\partial_y z$ affect the precession, including the rotational axis and precession angle. Now, we try to study two interesting

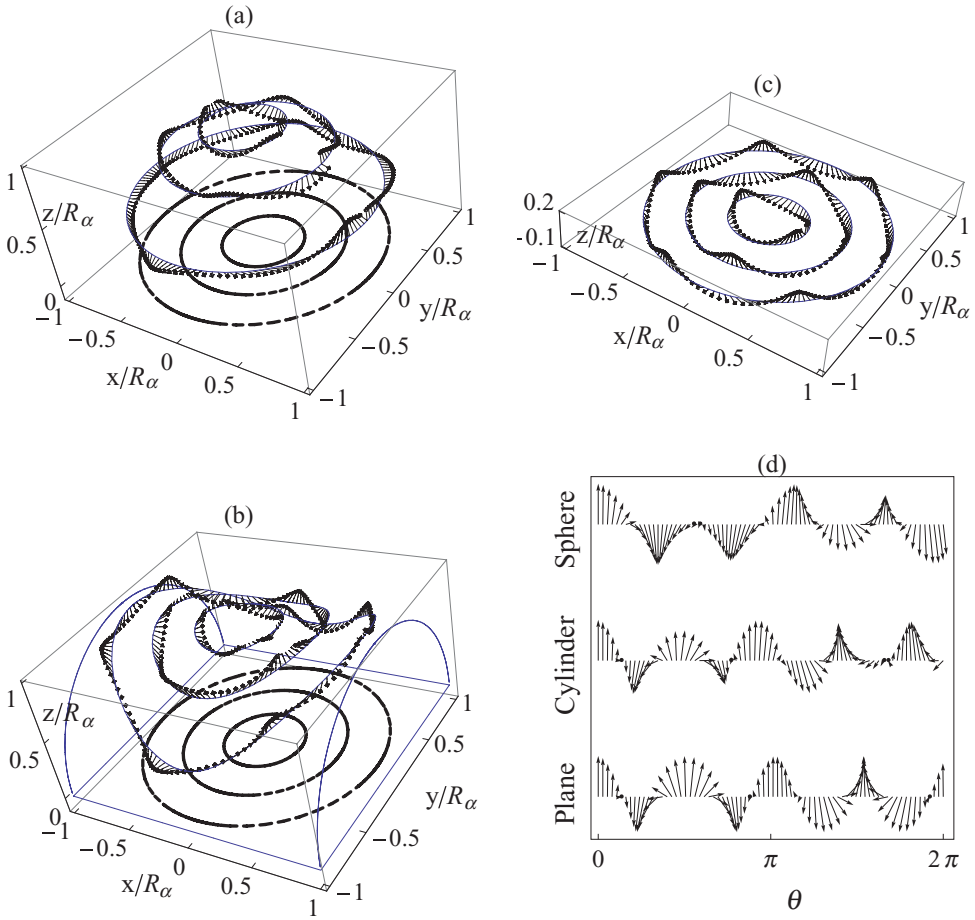

FIG. 7. (Color online) Precession with pure Rashba coupling on three types of surface, i.e., sphere (a), cylinder (b), and flat plane(c). The injected z-polarized electron moves along a closed loop with the same projective radius $r = 0.3R_\alpha, 0.6R_\alpha, 0.9R_\alpha$. The precession loops with $r = 0.6R_\alpha$ for the three different surfaces are given in (d) to clearly show the role of the space curvature.

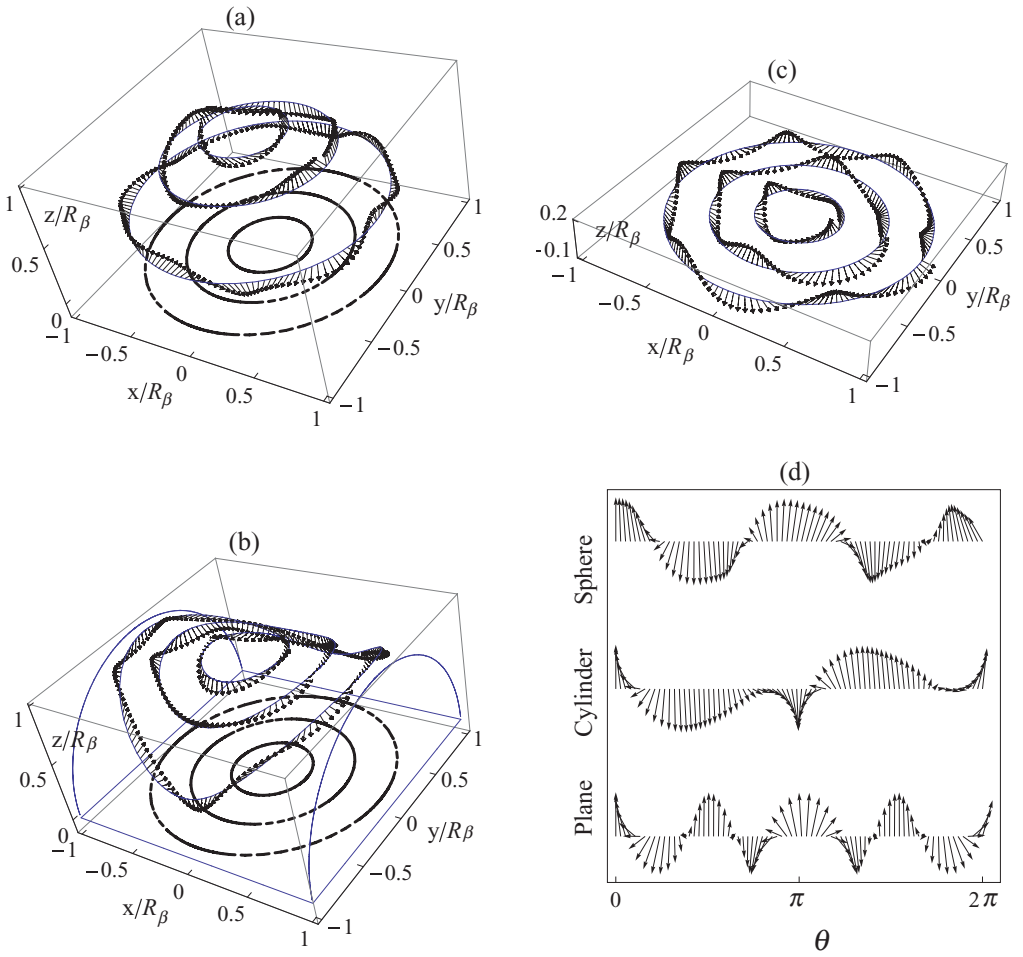

FIG. 8. (Color online) Precession with pure Dresselhaus coupling on three types of surface, i.e., sphere (a), cylinder (b), and flat plane (c). The injected z-polarized electron moves along a closed loop with the same projective radius $r = 0.3R_\beta, 0.6R_\beta, 0.9R_\beta$. The precession loops with $r = 0.6R_\beta$ for three different surfaces are given in (d) to clearly show the role of the space curvature.

examples: precession along a curved path and a closed loop on a 3D curved surface.

In several papers[11,14,39,41] spin precession was studied along many kinds of paths, such as straight wire, half ring, and square on a 2D x-y plane. In the first example, we generalize the precession path on a 3D curved surface. We study the spin precession along a curved path given by $z(x) = A\sin(\frac{\pi}{L}x)$; for simplicity but without loss of generality, the y direction is not included in the formula. With fixed initial and final positions and a constant L, by varying the parameter A, the curvature of the path can be easily changed. Injecting the z-polarized electron from the left, we can obtain the spin pattern and the final state along the different paths shown in Fig. 6. The unit vectors of the expection value of the spin $\frac{\langle s\rangle}{|\langle s\rangle|}$ at the end of path are $(0.56,0,-0.83)$, $(0.99,0,-0.16)$, $(0,0,1)$, $(0.99,0,-0.16)$, and $(0.56,0,-0.83)$ in Fig. 6(a) and $(0.25,0.92,-0.32)$, $(0.61,-0.59,0.54)$, $(0,0,1)$, $(-0.25,0.92,-0.32)$, and $(-0.61,-0.59,0.54)$ in Fig. 6(b), corresponding to $A = 2,1,0,-1,-2$, respectively. This case depends only on the longitudinal slope, and can be compared with previous cases in Sec. IV A . For a pure RSI ($\beta = 0$) [Fig. 6(a)], we know that the spin-rotation axis is independent of the path from Eq. (41), and is along the $-y$ direction. We also know that the change of precession angle with respect to x will increase as the slope increases from Eq. (42), namely, it is proportional to the travel distance. The case with pure DSI ($\alpha = 0$) is more complicated, and the precession axis changes with x on the x-z plane according to Eq. (44) [Fig. 6(b)]. From Fig. 6, even with the same initial condition of the injected electrons at the initial points, the spin orientation is quite different at the end points with different curvature. It is obvious that an extra phase is induced from the curvature of the curved space on the traveling electrons in addition to the spin-orbital interactions applicable on the flat space.

In the second example, we consider spin precession around a closed loop on a 3D curved surface. In the case with only RSI, the injected z-polarized electron moves around circles on the hemisphere, hemicyclinder, and plane with projective radius r. It starts from the position $x = R_\alpha$, $y = 0$, $z = z(x = R_\alpha, y = 0)$, and after rotating through 2π, returns to its original position. Thus, we can obtain the spin pattern along the path and the final state shown in

Fig. 7. The expectation values of the spin $\frac{\langle s\rangle}{|\langle s\rangle|}$ at the end of the path are [Fig. 7(a)] for the sphere $(0.57,-0.61,0.56)$, $(0.18,0.65,-0.74)$, and $(-0.23,-0.55,0.80)$, [Fig. 7(b)] for the cylinder $(-0.07,-0.94,-0.32)$, $(-0.63,-0.73,-0.26)$, and $(0.02,0.70,0.71)$, and [Fig. 7(c)] for the flat plane $(-0.18,-0.65,0.74)$, $(-0.03,0.57,0.82)$, and $(-0.16,0.99,-0.02)$ with projective radius $r = 0.3R_\alpha$, $0.6R_\alpha$, and $0.9R_\alpha$, respectively. Similarly, as shown in Fig. 8 with only DSI, the expectation values of the spin $\frac{\langle s\rangle}{|\langle s\rangle|}$ at the end of the path are [Fig. 8(a)] for the sphere $(0.30,-0.06,0.96)$, $(-0.82,-0.14,0.56)$, and $(-0.74,0.68,0.00)$, [Fig. 8(b)] for the cylinder $(0.04,0.99,0.11)$, $(0.25,-0.29,0.92)$, and $(-0.04,-0.04,0.99)$ and [Fig. 8(c)] for the flat plane $(-0.65,-0.18,0.74)$, $(0.57,-0.03,0.82)$, and $(0.99,-0.16,-0.02)$ with the projective radius $r = 0.3R_\alpha$, $0.6R_\alpha$, and $0.9R_\alpha$, respectively.

V. CONCLUSIONS

We have studied the curved-space-induced geometrical effect on spin-polarized electrons, and a general formalism of a single-particle Hamiltonian with the RSI and DSI on a curved surface is derived. We performed a gauge transformation to derive the spin-rotation operator and the analytical expression for the spin precession for ideally injected electrons with arbitrary spin polarization under both RSI and the DSI on a curved space. All geometric influences from curved space can be absorbed into a geometric tensor which induces an extra geometric phase on the spin-polarized electrons in addition to the conventional dynamic phase on a flat surface. Nevertheless, the spin-rotation axes of the geometric phase and dynamic phase are different. In particular, unique features of the spin-precession patterns, precession angles, and cone angles can be easily identified with the help of the spin-rotation operator. In general, the correction term from curved space cannot be removed from a particular gauge, but it can be effectively represented as an induced field B_{G1}. This curved-space-induced field is very different from the induced field from RSI and DSI and it will push the eigenspinor away from the x-y plane.

Our calculations explicitly demonstrate that the spin-orbital interaction in curved space can induce a geometrical field which will definitely affect the behavior of electrons with spin. Here we consider only the linear term in the momentum in RSI and DSI; in other words, the curved thin film is still assumed to be a 2D system and thus the cubic term in the momentum was neglected.[35,36] We only study the response of spin precession with an extra induced geometrical field as an example. The influences of the induced geometrical field on other physical properties of electrons with spin deserve further studies. Nevertheless, we have successfully shown that the curved-space-induced geometrical field is significant and cannot be neglected. The variation of the slope will usually affect both the rate of spin precession and the orientation axis. Closed loops on three types of geometry clearly show the difference of dynamics of the spin component along the conserving axis under a pure gauge SO coupling. Our qualitative analysis also indicates that variation of the curvature is a possible way to manipulate the spin motion. Therefore, in addition to use of magnetic and time-dependent electric fields to manipulate the spin electrons, the time dependence of space curvature can also be another easy tool of spin manipulation. Of course, our simple approach does not include some other deformation-related effects, but at least clearly shows the role of the space curvature based on the present Hamiltonian and thus the spin-orbital interaction.

Even though our analysis here considers only the single-particle picture, the interference of electrons along different paths will still be observed.[39,40] A possible experiment to test the validity of the geometrical effect of a curved space would involve an effect similar to the Aharonov-Bohm effect. For two half-ring-shaped stripes with different curvature of each half ring, interference will be observed for electrons with spin traveling along different paths. In addition to the normal Aharonov-Bohm effect, an extra phase shift should result from the difference of curvatures of the two half rings. In conclusion, we have derived an effective spin-orbit Hamiltonian for electrons in curved space. The curvature-induced effective geometrical field is determined by simple expressions, containing surface curvatures and the coupling constants α and β from Eqs. (22), (23), and (24). We believe that a geometric effective field would help to elucidate the profound physics of spin transport in spintronic devices with curved spaces, such as nanotubes and nanopillars.

ACKNOWLEDGMENT

The authors thank the National Science Council of the Republic of China for support under Grant No. NSC-98-2112-M-002-012-MY3.

APPENDIX A: DRESSELHAUS HAMILTONIAN ON A REDUCED TWO-DIMENSIONAL SURFACE

For a 3D Dresselhaus SO term,

$$H_D = \tfrac{1}{2}\vec{\sigma}\cdot\vec{\Omega}, \tag{A1}$$

where

$$\vec{\Omega}(k) = \frac{\eta\hbar^2}{(2m^3E_g)^{\frac{1}{2}}}\vec{\kappa} \tag{A2}$$

and

$$\vec{k} = \begin{pmatrix} k_x\left(k_y^2 - k_z^2\right) \\ k_y\left(k_z^2 - k_x^2\right) \\ k_z\left(k_x^2 - k_y^2\right) \end{pmatrix}, \tag{A3}$$

when an electron is within a thin film whose surface is $\vec{r} = (x,y,z(x,y))$. The unit vector along the normal to the surface is

$$\widehat{n} = (n_x,n_y,n_z) = \frac{(-\partial_x z,\partial_y z,1)}{[(\partial_x z)^2 + (\partial_y z)^2 + 1]^{-\frac{1}{2}}}. \tag{A4}$$

The momentum $\vec{k}$ of the electron can be written as $\vec{k} = \vec{p} + \vec{q}$ where $\vec{p}$ is the tangent to the surface; $\vec{q}$ is normal to the

surface. The electron is confined in the direction normal to the surface; the expection values in $\widehat{n}$ satisfy

$$\langle q_i \rangle = \langle q_i q_j q_k \rangle = 0, \quad \langle q_i q_j \rangle = \langle q^2 \rangle n_i n_j \tag{A5}$$

and the thickness of the surface is small. We have $\langle q^2 \rangle \gg k^2$ and set

$$k^3 \approx 0 \tag{A6}$$

within this paper. With the help of Eqs. (A5) and (A6),[36] the expectation value of the Hamiltonian in Eq. (A1) can be reduced to

$$H_D = \frac{\beta}{\hbar} \vec{\sigma} \cdot \vec{\chi}, \tag{A7}$$

where

$$\vec{\chi} = \begin{pmatrix} 2n_x(n_y p_y - n_z p_z) + \left(n_y^2 - n_z^2\right) p_x \\ 2n_y(n_z p_z - n_x p_x) + \left(n_z^2 - n_x^2\right) p_y \\ 2n_z(n_x p_x - n_y p_y) + \left(n_x^2 - n_y^2\right) p_z \end{pmatrix}. \tag{A8}$$

APPENDIX B: A GENERALIZED HAMILTONIAN IN CURVED SPACE

The Hamiltonian of Eq. (1) can be generalized into a curved surface of the form in Eq. (3). Einstein's summation and metric tensor are used in Eq. (3), and

$$g^{\mu\nu} = \begin{pmatrix} 1 + (\partial_x z)^2 & \partial_x z \partial_y z \\ \partial_x z \partial_y z & 1 + (\partial_y z)^2 \end{pmatrix}, \tag{B1}$$

which contains all the information about the geometry and is related to contravariant and covariant vectors, for example

$$p^\mu = g^{\mu\nu} p_\nu. \tag{B2}$$

The notation $\{\}_H$ is defined as

$$\left\{A_\mu, p^\mu\right\}_H = \tfrac{1}{2} A_\mu p^\mu + \tfrac{1}{2} p_\mu A^\mu. \tag{B3}$$

A_μ is given by

$$A_\mu = \sigma_i A_\mu^i, \tag{B4}$$

where

$$\begin{aligned}
A_\mu^1 = {} & \frac{mc}{e\hbar}\{\alpha(-\partial_x z \partial_y z)[(\partial_x z)^2 + (\partial_y z)^2 + 1]^{-\frac{1}{2}} + \beta[-1 + 2(\partial_x z)^2 + (\partial_y z)^2][(\partial_x z)^2 + (\partial_y z)^2 + 1]^{-1}, \\
& \alpha[-1 - (\partial_y z)^2][(\partial_x z)^2 + (\partial_y z)^2 + 1]^{-\frac{1}{2}} + \beta[4\partial_x z \partial_y z][(\partial_x z)^2 + (\partial_y z)^2 + 1]^{-1}\}, \\
A_\mu^2 = {} & \frac{mc}{e\hbar}\{\alpha[1 + (\partial_x z)^2][(\partial_x z)^2 + (\partial_y z)^2 + 1]^{-\frac{1}{2}} + \beta[-4\partial_x z \partial_y z][(\partial_x z)^2 + (\partial_y z)^2 + 1]^{-1}, \\
& \alpha(\partial_x z \partial_y z)[(\partial_x z)^2 + (\partial_y z)^2 + 1]^{-\frac{1}{2}} + \beta[1 - 2(\partial_y z)^2 - (\partial_x z)^2][(\partial_x z)^2 + (\partial_y z)^2 + 1]^{-1}\}, \\
A_\mu^3 = {} & \frac{mc}{e\hbar}\{\alpha(\partial_y z)[(\partial_x z)^2 + (\partial_y z)^2 + 1]^{-\frac{1}{2}} + \beta[-2\partial_x z + (\partial_x z)^3 - \partial_x z(\partial_y z)^2][(\partial_x z)^2 + (\partial_y z)^2 + 1]^{-1}, \\
& \alpha(-\partial_x z)[(\partial_x z)^2 + (\partial_y z)^2 + 1]^{-\frac{1}{2}} + \beta[2\partial_y z - (\partial_y z)^3 + \partial_y z(\partial_x z)^2][(\partial_x z)^2 + (\partial_y z)^2 + 1]^{-1}\}.
\end{aligned}$$

APPENDIX C: DISCRETE EVOLUTION OPERATOR FOR THE WAVE FUNCTION

The general solution of the differential equation

$$\frac{d}{ds}\varphi(s) = i\, O(s)\varphi(s) \tag{C1}$$

is

$$\varphi(s) = P \exp\left(i \int_0^s O(s')ds'\right)\varphi(0). \tag{C2}$$

Here the symbol P indicates the path order, and we discretized the path into N steps. We can obtain the discrete solution

$$\varphi(s) = P \prod_i^N [1 + i\, O(s_i)\, \Delta s]\varphi(0). \tag{C3}$$

Therefore, as long as N is large enough, we can obtain the approximate solution of $\varphi(s)$.

APPENDIX D: WILSON LOOP IN CURVED SPACE

Considering parallel transport around a closed path C, we choose C to be a parallelogram with one corner at r^μ and two sides dr^μ and δr^μ. The Wilson loop U_w is the product of four transports around the loop:[44]

$$\begin{aligned}
U_w = {} & U_G(r^\mu, r^\mu + dr^\mu) U_G(r^\mu + dr^\mu, r^\mu + dr^\mu + \delta r^\mu) \\
& \times U_G(r^\mu + dr^\mu + \delta r^\mu, r^\mu + \delta r^\mu) U_G(r^\mu + \delta r^\mu, r^\mu).
\end{aligned} \tag{D1}$$

Straightforward mathematics yields

$$U_w = \exp\left(\frac{ie}{\hbar c} F_{\mu\nu} dr^\mu \delta r^\nu\right) \tag{D2}$$

with field strength tensor

$$F_{\mu\nu} = D_\mu A_\nu - D_\nu A_\mu - \frac{ie}{\hbar c}[A_\mu, A_\nu], \tag{D3}$$

where D_μ is the covariant derivative. Thus, the results for the quantum ring[11,39] are special cases and can be derived easily.

In the case of slightly curved space, the Wilson loop turns out to be

$$U_w = \exp\left[\frac{ie}{\hbar c}(F_{0\mu\nu} + F_{G1\mu\nu})dx^\mu \delta x^\nu\right], \tag{D4}$$

where $F_{0\mu\nu}$ is the field strength tensor on flat space given by

$$\begin{aligned} F_{0\mu\nu} &= \sigma_i F^i_{0\mu\nu}, \\ F^1_{0\mu\nu} &= F^2_{0\mu\nu} = 0, \\ F^3_{0\mu\nu} &= \frac{2m^2c}{e\hbar^3}(\alpha^2 - \beta^2)\varepsilon_{\mu\nu}, \end{aligned} \tag{D5}$$

and $F_{G1\mu\nu}$ is the geometric contribution given by

$$\begin{aligned} F_{G1\mu\nu} &= \sigma_i F^i_{G1\mu\nu}, \\ F^1_{G1\mu\nu} &= \frac{2m^2c}{e\hbar^3}[(-\alpha^2 + 2\beta^2)\partial_x z + \alpha\beta\partial_y z]\varepsilon_{\mu\nu}, \\ F^2_{G1\mu\nu} &= \frac{2m^2c}{e\hbar^3}[\alpha\beta\partial_x z + (-\alpha^2 + 2\beta^2)\partial_y z]\varepsilon_{\mu\nu}, \\ F^3_{G1\mu\nu} &= \frac{2m^2c}{e\hbar^3}\left[-\alpha\left(\partial_x^2 z + \partial_y^2 z\right) + 2\beta\partial_x\partial_y z\right]\varepsilon_{\mu\nu}. \end{aligned} \tag{D6}$$

*crchang@phys.ntu.edu.tw

[1] I. Zutic, J. Fabian, and S. Das Sarma, Rev. Mod. Phys. **76**, 323 (2004).
[2] D. D. Awschalom and M. E. Flatte, Nat. Phys. **3**, 153 (2007).
[3] E. I. Rashba, Sov. Phys. Solid State **2**, 1109 (1960).
[4] Yu. A. Bychkov and E. I. Rashba, JETP Lett. **39**, 78 (1984).
[5] J. Nitta, T. Akazaki, H. Takayanagi, and T. Enoki, Phys. Rev. Lett. **78**, 1335 (1997).
[6] T. Koga, J. Nitta, T. Akazaki, and H. Takayanagi, Phys. Rev. Lett. **89**, 046801 (2002).
[7] S. Datta and B. Das, Appl. Phys. Lett. **56**, 665 (1990).
[8] Ming-Hao Liu and Ching-Ray Chang, Phys. Rev. B **73**, 205301 (2006).
[9] G. Dresselhaus, Phys. Rev. **100**, 580 (1955).
[10] P. Q. Jin, Y. Q. Li, and F. C. Zhang, J. Phys. A **39**, 7115 (2006).
[11] N. Hatano, R. Shirasaki, and H. Nakamura, Phys. Rev. A **75**, 032107 (2007).
[12] C. N. Yang and R. Mills, Phys. Rev. **96**, 191 (1954).
[13] M. V. Berry, Proc. R. Soc. London, Ser. A **392**, 45 (1984).
[14] Son-Hsien Chen and Ching-Ray Chang, Phys. Rev. B **77**, 045324 (2008).
[15] Jyh-Shinn Yang, Xiao-Gang He, Son-Hsien Chen, and Ching-Ray Chang, Phys. Rev. B **78**, 085312 (2008).
[16] V. P. Mineev and G. E. Volovik, J. Low Temp. Phys. **89**, 823 (1992).
[17] J. Frohlich and U. M. Studer, Rev. Mod. Phys. **65**, 733 (1993).
[18] I. L. Aleiner and V. I. Fal'ko, Phys. Rev. Lett. **87**, 256801 (2001).
[19] L. S. Levitov and E. I. Rashba, Phys. Rev. B **67**, 115324 (2003).
[20] K. C. Nowack, F. H. L. Koppens, Yu. V. Nazarov, and L. M. K. Vandersypen, Science **318**, 1430 (2007).
[21] Q. Liu, T. Ma, and S. C. Zhang, Phys. Rev. B **76**, 233409 (2007).
[22] S. R. Eric Yang, Phys. Rev. B **75**, 245328 (2007).
[23] I. V. Tokatly and E. Ya. Sherman, Ann. Phys. **325**, 1104 (2010).
[24] S. R. Eric Yang and N. Y. Hwang, Phys. Rev. B **73**, 125330 (2006).
[25] I. V. Tokatly, Phys. Rev. Lett. **101**, 106601 (2008).
[26] Ming-Hao Liu and Ching-Ray Chang, Phys. Rev. B **74**, 195314 (2006).
[27] L. I. Magarill, D. A. Romanov, and A. V. Chaplik, JETP Lett. **64**, 460 (1996).
[28] M. Trushin and J. Schliemann, New J. Phys. **9**, 346 (2007).
[29] Chien-Liang Chen, Son-Hsien Chen, Ming-Hao Liu, and Ching-Ray Cheng, J. Appl. Phys. **108**, 033715 (2010).
[30] V. V. Rotkin and R. A. Suris, Phys. Solid State **36**, 1899 (1994).
[31] H. Aoki and H. Suezawa, Phys. Rev. A **46**, R1163 (1992).
[32] L. I. Magarill, D. A. Romanov, and A. V. Chaplik, Zh. Eksp. Teor. Fiz. **113**, 1411 (1998); L. I. Magarill and A. V. Chaplik, *ibid.* **115**, 1478 (1999) [JETP **88**, 815 (1999)].
[33] M. V. Entin and L. I. Magarill, Phys. Rev. B **64**, 085330 (2001).
[34] Roland Winkler, *Spin-Orbital Coupling Effect in Two-Dimensional Electron and Hole Systems* (Springer, Berlin, 2003).
[35] M. I. D'yakonov and V. I. Perel, Sov. Phys. JETP **33**, 1053 (1971).
[36] M. I. D'yakonov and V. Y. Kachorovskii, Sov. Phys. Semicond. **20**, 110 (1986).
[37] A. Bohm, A. Mostafazadeh, H. Koizumi, Q. Niu, and J. Zwanziger, *The Geometric Phase in Quantum Systems* (Springer, Berlin, 2003).
[38] David J. Griffiths, *Introduction to Quantum Mechanics* (Prentice-Hall, Englewood Cliffs, NJ, 2004).
[39] Ming-Hao Liu, Kuo-Wei Chen, Son-Hsien, and Ching-Ray Chang, IEEE Trans. Magn. **43**, 2869 (2007).
[40] Takaaki Koga, Yoshiaki Sekine, and Junsaku Nitta, Phys. Rev. B **74**, 041302(R) (2006).
[41] A. M. Lobos and A. A. Aligia, Phys. Rev. Lett. **100**, 016803 (2008).
[42] M. P. Hobson, G. P. Efstathiou, and A. N. Lasenby, *General Relativity* (Cambridge University Press, Cambridge, 2006).
[43] A. B. Vorob'ev, V. Ya. Prinz, Yu. S. Yu. S. Yukecheva, and A. I. Toropov, Physica E **23**, 171 (2004).
[44] Tai-Peei Cheng and Ling-Fong Li, *Gauge Theory of Elementary Particle Physics* (Oxford University Press, Oxford, 2000).